

Magnetic order in the periodic Anderson model

B. Möller and P. Wölfle

*Institut für Theorie der Kondensierten Materie,
Physikhochhaus, Universität Karlsruhe, 76128 Karlsruhe, Federal Republic of Germany*

(Received 26 May 1993)

We study the ground state of the symmetric, finite- U , periodic Anderson model using a mean-field slave-boson theory of the Kotliar-Ruckenstein type. At half filling (two electrons per site) we find a charge gap at all $U > 0$ and a transition from the paramagnetic to an antiferromagnetically ordered (AF) state at a critical value of the on-site interaction U for given hybridization V . The AF state is found to be lowest in energy within the manifold of spiral magnetic states. Results for the energy, hybridization matrix element, and local moment compare well with quantum Monte Carlo results for finite systems. Lowering the density induces a smooth crossover from AF to ferromagnetic (F) order via a spiral phase. Closely above $\frac{1}{4}$ filling a first order transition from F to AF order is found. The insulating state at $\frac{1}{4}$ filling is shown to be described by an AF Heisenberg model.

I. INTRODUCTION

The periodic Anderson model (PAM) is thought to describe the essential physics of many transition-metal, rare-earth and actinide metallic compounds including the so-called heavy-fermion systems.¹ The model has also been proposed to describe the cuprate superconductors. It is one of the archetypical models of correlated fermions on a lattice, consisting of a band of "light," uncorrelated electrons coupled to a band of heavy strongly correlated electrons. Despite intense efforts to determine the properties of the model, controlled results are scarce and many questions remain. For one, the well-known physics of the single-impurity Anderson model,² i.e., the formation of magnetic moments and their screening by the Kondo effect is expected to prevail for sufficiently large exchange coupling J of the conduction electrons to the local moments. On the other hand, for small values of J the local moments are expected to order, in most cases antiferromagnetically, at temperatures far above the Kondo temperature, such that the Kondo effect is prohibited by the presence of the strong antiferromagnetic local field.³ It has proved to be difficult to incorporate these two opposing trends in any theoretical formulation. Methods that have been used for the single impurity case to obtain analytically exact results like the Bethe-ansatz method^{4,5} or numerically exact results using Wilson's renormalization-group transformation⁶ cannot be generalized to the lattice case. A different and less well explored regime is that of small density of electrons in the conduction band and a singly occupied low-lying f level. For this case ferromagnetic order has been predicted recently.^{7,8}

Over the past few years new powerful analytical tools have been developed, which may allow a qualitatively correct description of correlated Fermi systems. These are the so-called slave boson theories, which make use of auxiliary particles to effect the bookkeeping of site occupations required in any lattice model with strong on-site interaction. The initially proposed slave-boson

representations⁹⁻¹¹ use only one scalar slave-boson (in the infinite repulsion limit) and are able to provide a qualitatively correct account of the Kondo effect. However, the slave boson being a spin scalar, the antiferromagnetic interaction between local moments is not easily recovered in this language. The alternative is a slave boson representation employing spin-carrying slave bosons, like the representation introduced by Kotliar and Ruckenstein¹² and its symmetry-conserving generalizations.¹³ We shall use the latter method in this paper. In particular, we will discuss the paramagnetic and spiral magnetic mean-field solutions, the latter including antiferromagnetic and ferromagnetic states as well. Since there is no small parameter in this strong-coupling theory (except for $1/N$ in N -orbital generalization of the model), there is no obvious inherent quality criterion available. We therefore rely on comparison with numerically exact results for finite-size systems.

II. MODEL AND METHOD

In this paper we will study the Anderson lattice model with two orbitals per site and spin degeneracy $N = 2$, defined by the Hamiltonian

$$H = -t \sum_{\langle ij \rangle, \sigma} c_{i\sigma}^\dagger c_{j\sigma} + V \sum_{i, \sigma} (c_{i\sigma}^\dagger f_{i\sigma} + \text{H.c.}) + \epsilon_f \sum_{i, \sigma} n_{i\sigma}^f + U \sum_i n_{i\uparrow}^f n_{i\downarrow}^f. \quad (1)$$

Here the $c_{i\sigma}^\dagger$ and $f_{i\sigma}^\dagger$ create electrons in conduction electron and f electron Wannier states at site i with spin projection σ . t is the conduction-electron nearest-neighbor hopping element and $\langle ij \rangle$ denotes a pair of nearest neighbors, V is the on-site hybridization matrix element, ϵ_f is the energy of the f orbital and U is the Coulomb interaction matrix element for two electrons with spins \uparrow, \downarrow

occupying the same Wannier state. In the limit of large U , the interaction term is the dominating term in Eq. (1). It is therefore useful to introduce a representation of the f electron operators in terms of auxiliary particles, which serves to linearize the Coulomb interaction terms. In the following we will use the slave-boson representation introduced by Kotliar and Ruckenstein¹² and generalized in Ref. 13. Within this formulation the f -electron field operators are represented by a combination of $S = \frac{1}{2}$ pseudofermion operators $s_{i\sigma}$ and scalar slave-boson operators e, d, p_o for the empty, doubly occupied as well as the charge part of the singly occupied states and a three component vector operator $\mathbf{p} = (p_1, p_2, p_3)$ for the spin part of the singly occupied state:

$$f_{i\sigma} = \sum_{\sigma'} z_{i\sigma\sigma'} s_{i\sigma'}, \quad \sigma = \uparrow, \downarrow, \quad (2)$$

where

$$\underline{z} = e^\dagger \underline{L} M \underline{R} p + \underline{p}^\dagger \underline{L} M \underline{R} d$$

and

$$\begin{aligned} \underline{L} &= \left[(1 - d^\dagger d) \underline{1} - 2 \underline{p}^\dagger \underline{p} \right]^{-1/2}, \\ \underline{R} &= \left[(1 - e^\dagger e) \underline{1} - 2 \underline{p}^\dagger \underline{p} \right]^{-1/2}, \\ M &= \left[1 + e^\dagger e + d^\dagger d + \sum_{\mu} p_{\mu}^\dagger p_{\mu} \right]^{1/2}. \end{aligned} \quad (3)$$

Here $\underline{z}, \underline{L}, \underline{R}$ are 2×2 spin matrices and $p_{\sigma\sigma'} = \frac{1}{2} \sum_{\mu} p_{\mu} \tau_{\mu, \sigma\sigma'}$, with $\tau_{\mu}, \mu = 1, 2, 3$, the Pauli matrices and τ_0 the unit matrix. The slave particle operators are subject to the constraints

$$\begin{aligned} e_i^\dagger e_i + d_i^\dagger d_i + \sum_{\mu} p_{i\mu}^\dagger p_{i\mu} &= 1, \\ s_{i\sigma}^\dagger s_{i\sigma} &= 2 \sum_{\sigma_1} p_{i\sigma_1}^\dagger p_{i\sigma_1} + \delta_{\sigma\sigma'} d_i^\dagger d_i, \\ \mathbf{p}_i^\dagger \times \mathbf{p}_i &= \mathbf{0}. \end{aligned} \quad (4)$$

In terms of the auxiliary operators the Anderson Hamiltonian (1) takes the form

$$\begin{aligned} H = \sum_i \left\{ -t \sum_{\tau\sigma} (c_{i+\tau\sigma}^\dagger c_{i\sigma} + \text{H.c.}) + V \sum_{\sigma\sigma'} (c_{i\sigma}^\dagger z_{i\sigma\sigma'} s_{i\sigma'} + \text{H.c.}) + U d_i^\dagger d_i + \alpha_i \left(e_i^\dagger e_i + d_i^\dagger d_i + \sum_{\mu} p_{i\mu}^\dagger p_{i\mu} - 1 \right) \right. \\ \left. + \beta_{i0} \left(\sum_{\sigma} s_{i\sigma}^\dagger s_{i\sigma} - \sum_{\mu} p_{i\mu}^\dagger p_{i\mu} - 2 d_i^\dagger d_i \right) + \beta_i \cdot \left(\sum_{\sigma\sigma'} \tau_{\sigma\sigma'} s_{i\sigma}^\dagger s_{i\sigma} - p_{i0}^\dagger \mathbf{p}_i - \mathbf{p}_i^\dagger p_{i0} \right) + \gamma_i (\mathbf{p}_i^\dagger \times \mathbf{p}_i) \right\}. \end{aligned} \quad (5)$$

The quantities $\alpha_i, \beta_{i\mu}$, and $\gamma_{i\mu}$ are Lagrange multiplier fields (for details of the method see Ref. 13).

The system of interacting fermions and bosons described by Eq. (5) does not appear to pose a simpler problem than the original one. However, mean-field approximations on the slave-boson Hamiltonian are more likely to capture the essential physics of the model than Hartree-Fock theory on the original electron Hamiltonian does. The simplest mean-field theory is obtained by assuming all Bose and Lagrange multiplier fields to be space- and time-independent averages. Assuming a paramagnetic state, this leads to the so-called Gutzwiller approximation discussed in Ref. 14, by Varma, Weber, and Randall,¹⁵ and others.^{16,17} At first sight, a surprising feature of this solution is that the characteristic energy scale T_k^* obtained in this approximation is not given by the single impurity Kondo temperature, $T_K \sim W \exp[-U/4V^2 N(\epsilon_F)]$ as might have been expected [W is the bandwidth and $N(\epsilon_F)$ the density of states (DOS) of conduction electrons at the Fermi level] but rather by something like the square root of this. Whether this is an artifact of the approximation or rather represents a true feature of the lattice model as opposed to the impurity model, as has been argued,¹⁴ remains to be seen. Some support for the latter view comes from interpretation of quantum Monte Carlo results for a finite Anderson lattice.¹⁸

In this paper we study the spiral magnetic mean-field solutions of Eq. (5) for the case of a hypercubic lattice. This is defined by taking the spin-independent fields $e_i, p_{0i} d_i, \alpha_i$ to be spatially uniform, but assuming a spiral magnetic pattern for the spin-dependent fields $\mathbf{p}_i = p(\cos \phi_i, \sin \phi_i, 0)$, $\phi_i = \mathbf{q} \cdot \mathbf{R}_i$, where \mathbf{R}_i is the position vector of lattice site i and similarly $\beta_i = \beta(\cos \phi_i, \sin \phi_i, 0)$. The mean-field Hamiltonian then takes the form

$$\begin{aligned} H - \mu N &= \sum_{\mathbf{k}} X_{\mathbf{k}}^\dagger \mathcal{E}_{\mathbf{k}} X_{\mathbf{k}} \\ &+ N_L \{ U d^2 - \beta_0 (p_0^2 + p^2 + 2d^2) \\ &+ 2\beta p_0 p + \alpha (d^2 + e^2 + p^2 + p_0^2 - 1) \}, \end{aligned} \quad (6)$$

where N_L is the number of lattice sites and μ is the chemical potential. The first term involves a sum over wave vectors in the first Brillouin zone, and $X_{\mathbf{k}} = (c_{\mathbf{k}\uparrow}, s_{\mathbf{k}\uparrow}, c_{\mathbf{k}+\mathbf{q}\downarrow}, s_{\mathbf{k}+\mathbf{q}\downarrow})$ is a four-component spinor field. The energy matrix $\mathcal{E}_{\mathbf{k}}$ is defined as

$$\mathcal{E}_{\mathbf{k}} = \begin{pmatrix} \epsilon_{\mathbf{k}} - \mu & Vz_+ & 0 & Vz_- \\ Vz_+ & \epsilon_f + \beta_0 - \mu & Vz_- & -\beta \\ 0 & Vz_- & \epsilon_{\mathbf{k}+\mathbf{q}} - \mu & Vz_+ \\ Vz_- & -\beta & Vz_+ & \epsilon_f + \beta_0 - \mu \end{pmatrix}, \quad (7)$$

where

$$z_{\pm} = \frac{ep_{+} + dp_{-}}{\sqrt{1-d^2-p_{+}^2}\sqrt{1-e^2-p_{-}^2}} \pm \frac{ep_{-} + dp_{+}}{\sqrt{1-d^2-p_{-}^2}\sqrt{1-e^2-p_{+}^2}} \quad (8)$$

and $\epsilon_k = -2t \sum_{\nu=1}^d \cos(k_{\nu}a)$ is the dispersion of the conduction band. The mean-field parameters $e, d, p, p_0, p_{\pm} = p_0 \pm p$ and α, β_o, β are determined by requiring that the mean-field-free energy

$$F = -T \sum_{\mathbf{k}, \sigma, \alpha} \ln[1 + \exp(-E_{\mathbf{k}\sigma\alpha}/T)] + N_L[Ud^2 - \beta_o(p_0^2 + p^2 + 2d^2) + 2\beta p_0 p] \quad (9)$$

be stationary. Here $p = (1-d^2-e^2-p_0^2)^{1/2}$ is used, eliminating the first constraint. The quantities $E_{\mathbf{k}\sigma\alpha}$, where $\sigma = \uparrow, \downarrow$ labels the spin and $\alpha = \pm$ is a band index, are the four eigenvalues of the energy matrix \mathcal{E}_k . We note that F is minimum with respect to variations of the ‘‘internal’’ degrees of freedom e, d, p_0 but is maximum with respect to the ‘‘external’’ fields β, β_o . The stationarity condition on F is expressed by the saddle point equations

$$\frac{\partial F}{\partial e} = \frac{\partial F}{\partial d} = \frac{\partial F}{\partial p_0} = \frac{\partial F}{\partial \beta} = \frac{\partial F}{\partial \beta_o} = 0. \quad (10)$$

III. NUMERICAL RESULTS OF MEAN-FIELD THEORY

We have determined the stationary point of the free energy Eq. (9) numerically at zero temperature and for a hypercubic lattice in dimensions $d = 1, 2, 3$, in the symmetric limit $\epsilon_f = -U/2$. The hybridization parameter was chosen as $V = 0.375t \cdot 2$, which is small compared to the bandwidth $W = 4dt$. All values of U to be quoted later will be in units of $2t$. Rather than solving the saddle-point equations, we minimized and maximized F in the subspaces of physical and Lagrange parameters, respectively.

We first consider the case of half filling, i.e., two electrons per site. We find that if magnetic ordering occurs, the antiferromagnetic state is most stable within the manifold of spiral states in the parameter space considered. An instability of the paramagnetic state with respect to magnetic order has been anticipated in Ref. 14. In particular within the framework of variational calculations the ferromagnetic state has been considered recently in Ref. 19, whereas antiferromagnetic order was considered in Refs. 20–22.

In Fig. 1 the scaled ground-state energy for $d = 1$ dimension is shown as a function of U . The result of the present calculation (solid line) is seen to compare well with quantum Monte Carlo results (circles) by Blankenbecler *et al.* (Ref. 23). For comparison, we also show the result for the paramagnetic mean-field solution (dashed-dotted line). The uppermost curve (double-dot-dashed

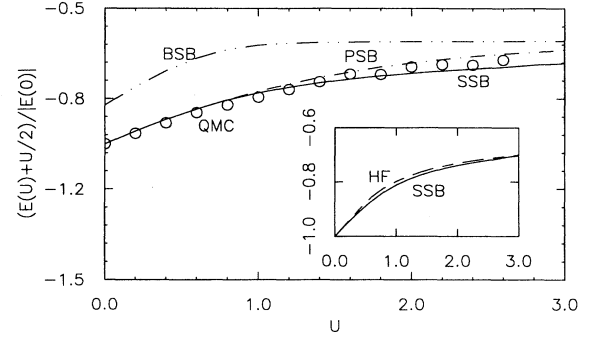


FIG. 1. Scaled ground-state energy of the PAM at half filling ($n = 2$) versus $(U/2t)$ for $d = 1$ dimension ($t = 0.5, V = 0.375t \cdot 2$); this work (—); paramagnetic Gutzwiller approximation (— · — · —); simple slave-boson theory (— · · —); inset: comparison with AF Hartree Fock.

line) is the result of the simple slave-boson mean-field theory, Refs. 10 and 11.

In Fig. 2 the average of the square of the local magnetization $\langle m_z^2 \rangle$ for $d = 1$ is plotted versus U . Again our result for the antiferromagnetic phase (solid line) follows the quantum Monte Carlo (QMC) data closely. The limiting behavior for weak (···) and strong coupling is also shown, as is the result for the paramagnetic phase. The simple slave-boson theory is again far off.

In Fig. 3 the effective hopping transition element onto the localized f level is shown for $d = 1$. This is a more sensitive quantity than the ground-state energy. Our result follows the QMC data fairly well, while the paramagnetic result is substantially off. The simple slave-boson theory fails badly for this quantity.

Next, we determined the magnetic phase diagram in the $V^2 - U$ plane for half filling and for hypercubic lattices in $d = 1, 2, 3$ dimension, as shown in Fig. 4. In one dimension there is of course no true long-range order. There the mean-field description should be taken as simulating short-range magnetic order, which apparently con-

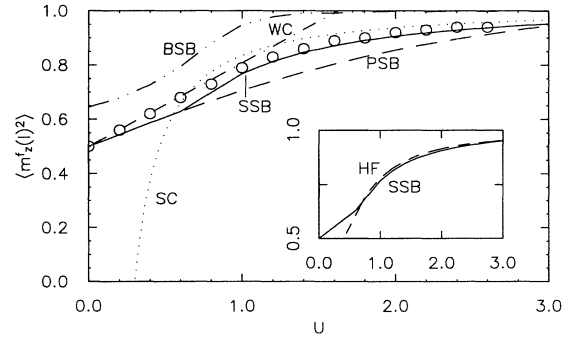


FIG. 2. Average of the squared local magnetization versus $(U/2t)$ for $d = 1$ ($t = 0.5, V = 0.375t \cdot 2, n = 2$). This work (—); paramagnetic Gutzwiller approximation (— · — · —); simple slave boson theory (— · · —); strong-coupling expansion (···); weak coupling expansion (— · —); inset: comparison with AF Hartree Fock.

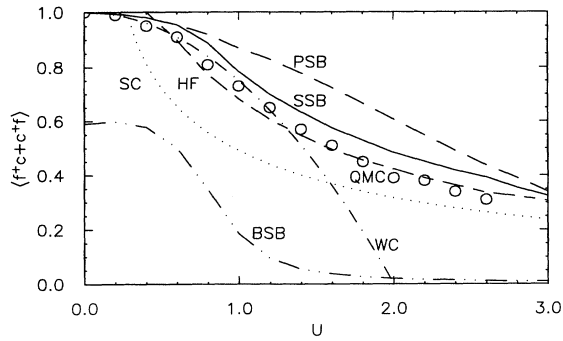


FIG. 3. Average of the hybridization operator versus $(U/2t)$ for $d = 1$ ($t = 0.5, V = 0.375t \cdot 2, n = 2$). Coding of curves as in Fig. 2.

tributes to the ground-state energy in an important way. The phase boundary is roughly linear, indicating that the transition occurs at a critical value of the exchange coupling constant $J = V^2[1/|\epsilon_f| + 1/(U + \epsilon_f)] = 4V^2/U$, $J_c \cong 0.036W$ in $d = 3$ dimensions. This is in qualitative agreement with the behavior of the corresponding Kondo lattice, for which a transition between the Kondo screened paramagnetic Fermi-liquid state and antiferromagnetically ordered state has been predicted Ref. 3 when the Kondo energy scale $T_K \sim W \exp(-W/J)$ is equal to the Ruderman-Kittel-Kasuya-Yosida (RKKY) spin interaction scale $I \sim J^2/W$. The value of J_c appears to be somewhat higher, as a consequence of the higher-energy scale T_k^* characterizing the paramagnetic state in this approximation.

Our critical value for J is close to the value obtained by a Gutzwiller-type variational solution of the Kondo lattice model.²⁴ The above results at half filling are very close to, or possibly even identical to, those of a recent variational calculation for the PAM employing the Gutzwiller approximation applied to a general antiferromagnetic state of the noninteracting system.²² Also shown is the result of a Hartree-Fock calculation, which

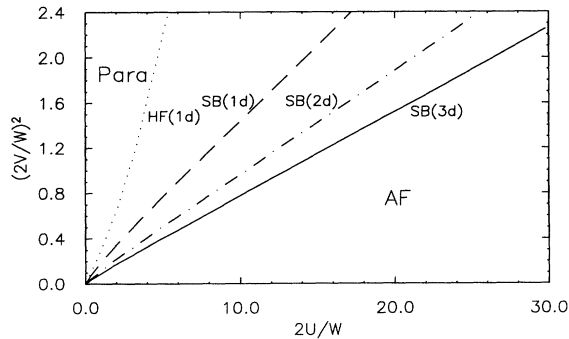


FIG. 4. Phasediagram of the PAM at half filling ($n=2$) in the $(2V/W)^2$ versus $2U/W$ plane. The phase boundary separating paramagnetic and antiferromagnetic phases according to our work for $d = 1$ (—), $d = 2$ (---), and $d = 3$ (—) dimensions is shown together with the Hartree-Fock result (···).

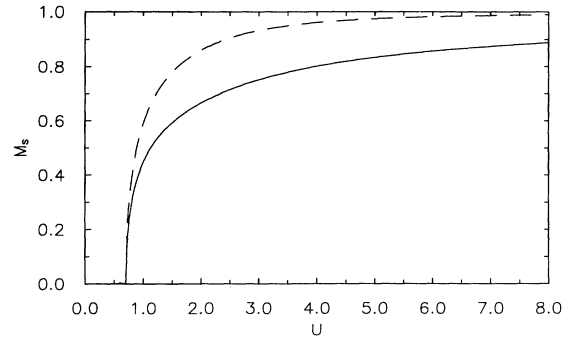


FIG. 5. Sublattice magnetization M_s versus $U/2t$ for $d = 1$ ($t = 0.5, V = 0.375t \cdot 2, n = 2$). f -electron contribution (---) and total magnetization (—) is shown.

is seen to badly overestimate the antiferromagnetic (AF) region.

The sublattice magnetization M_s of the f -electron system and of the combined f -electron and conduction-electron system in $d = 1$ dimension is shown in Fig. 5. M_s is seen to rise very rapidly and to attain values close to saturation for $U/2t \gtrsim 6$, approaching the limiting value of $M_s = 1$ as $1/U$. The conduction-electron contribution to M_s is seen to be negative and small, compensating part of the f -electron polarization.

Figure 6 shows the charge gap as a function of U in $d = 1$ dimension. The gap is determined from the quasiparticle band structure, which has two bands, the lower band being filled at half filling. Doping holes into the lower band immediately leads to a metallic state. The behavior at large U is given by $E_{\text{gap}} = 2z_+^2 V^2 / \beta \sim 1/U$.

We now turn to densities away from half filling, down to $\frac{1}{4}$ filling. For parameters such that the ground state is antiferromagnetically ordered at half filling we find that upon doping with holes the magnetic wave vector q decreases from its value $q = \pi$ ($d = 1$) linearly with the doping concentration (Fig. 7). In other words, the antiferromagnetic phase transforms into an incommensurate spiral phase. At a critical value of density $n_c(U)$, q is found to vanish, indicating a continuous transition to a ferromagnetic state.

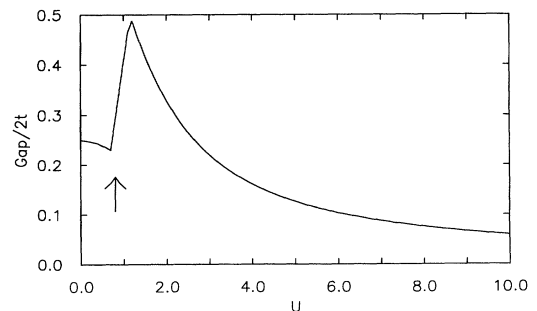


FIG. 6. Charge excitation gap in $d = 1$ in units of $2t$ versus $U/2t$ ($t = 0.5, V = 0.375t \cdot 2, n = 2$). The paramagnetic to antiferromagnetic phase transition is indicated by the arrow.

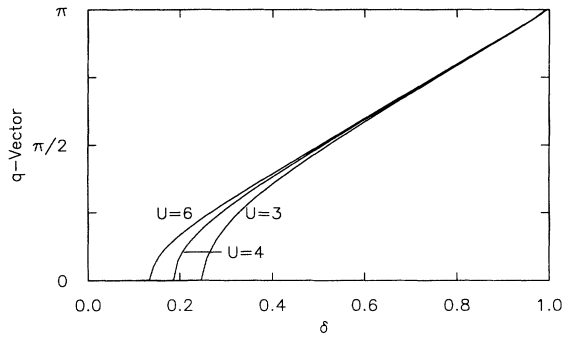


FIG. 7. Wave vector Q of the spiral magnetic order parameter in $d = 1$ in units of $(\text{lattice constant})^{-1}$ versus concentration of electrons δ in the conduction band, for various values of $U/2t$ ($t = 0.5, V = 0.375t \cdot 2$).

In Fig. 8, the length of the spiral magnetization vector is plotted as a function of density for various U . One observes that the ferromagnetism is not saturated, but increases towards saturation as the density is lowered (see next section). The ferromagnetic phase found here is not unexpected, as a ferromagnetic phase at and above $\frac{1}{4}$ filling has been predicted for the Kondo-lattice model Refs. 7 and 8. What is surprising at first sight, however, is that we find the antiferromagnetic solution to be stable at $\frac{1}{4}$ filling and in a small region of densities above $N = 1$. This is shown in the phase diagram Fig. 9. The transition from antiferromagnetism to ferromagnetism is of first order. A very similar phase diagram is obtained in Hartree-Fock theory. The reason for antiferromagnetic order at $\frac{1}{4}$ filling and ferromagnetic order for somewhat higher filling factors will be discussed in the next section.

To conclude the presentation of numerical results we show in Fig. 10 the occupation of the local level as a function of density for various values of U . As to be expected n_f is close to unity and increases with increasing U . Phase separation is not an issue for this model (in contrast to the Hubbard model), as can be inferred from the monotonical behavior of the chemical potential with density shown in Fig. 11.

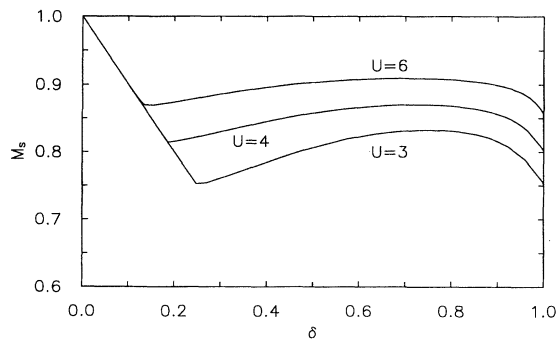


FIG. 8. Total magnitude of spiral magnetization versus conduction electron density δ for various values of $U/2t$.

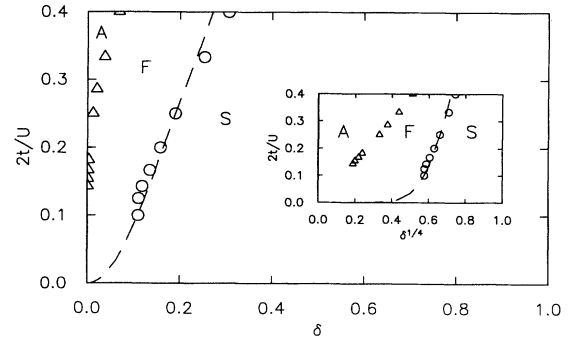


FIG. 9. Phase diagram in the $2t/U$ versus δ plane at $T = 0$. Spiralmagnetic, ferromagnetic, and antiferromagnetic regions are indicated. The inset shows the behavior near $\delta = 0$.

IV. ANTIFERROMAGNETIC AND FERROMAGNETIC ORDER AT AND NEAR $\frac{1}{4}$ FILLING

In the case that the local level ϵ_f is far below the conduction band, i.e., for $U \gg W$ in the symmetric case, where W is the conduction-band width, we can expect the local f states to be exactly singly occupied for $\frac{1}{4}$ filling (one electron per site). We have an insulating state of the charge transfer type, with a gap in the charge excitation spectrum $E_g = \frac{1}{2}(U - W)$. The manifold of ground states defined in this way is highly degenerate with respect to the spin configuration. As usual, spin exchange interactions mediated by virtual transitions into charge excited states will remove the degeneracy. The lowest-order exchange process involves excitation into the conduction band, hopping to a nearest-neighbor site and de-excitation into the local level, for both of the exchanged electrons, e.g., a sixth-order process. The effective Hamiltonian is that of the antiferromagnetic isotropic $S = \frac{1}{2}$ Heisenberg model

$$H = J_A \sum_{\langle ij \rangle} \mathbf{S}_i \cdot \mathbf{S}_j . \quad (11)$$

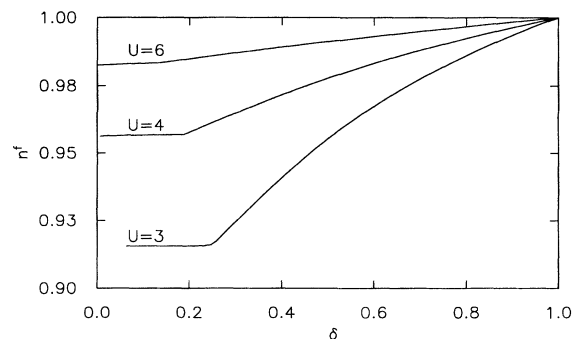


FIG. 10. Occupation number of the f -level versus δ for various $U/2t$ values.

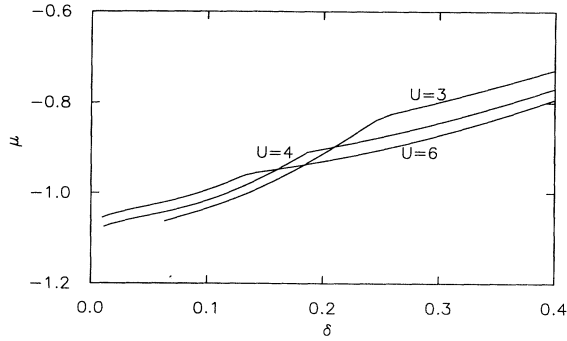


FIG. 11. Chemical potential versus δ for various $U/2t$.

In the limit $|\epsilon_f| = U/2 \gg t, V$, the exchange constant is found as $J_A \sim t^2 V^4 / |\epsilon_f|^5$. (For a discussion of the hopping expansion in the PAM see also Ref. 25.)

Additional electrons have to go into the conduction band. Analysis of the atomic energy states shows that the ground state of the two electron system is a spin singlet of energy

$$E_S = \frac{1}{2} \left[\epsilon_f - (\epsilon_f^2 + 16V^2)^{1/2} \right] \simeq \epsilon_f - \frac{4V^2}{|\epsilon_f|}. \quad (12)$$

The first excited state is a spin triplet at $E_T = \epsilon_f$ and the remaining two states are at energy $E \sim 0$. For low density such that the Fermi energy in the E_S band is less than $E_T - E_S$ the singlet pairs are tightly bound and move in the spin background of the unpaired localized spins. This situation is reminiscent of the t - J model, if the singlets are identified with the holes doped into the half-filled band and J_A is identified with the exchange interaction J there. The kinetic energy of the holes is minimized for a ferromagnetic background. The energy gain per site ΔE_F in the ferromagnetic state as compared to the paramagnetic state is of the order of the singlet to triplet excitation energy per singlet or $\Delta E_F \sim 4(V^2 / |\epsilon_f|) \delta$, where $\delta = n - 1$. This has to be compared with the energy gain in the antiferromagnetic state induced by direct exchange interaction $\Delta E_{AF} \sim J_A$. The phase transition from the AF to the F state is expected to occur when $\Delta E_F \sim \Delta E_{AF}$, or

$$\frac{t^2}{\epsilon_f^2} = C_F \frac{\epsilon_f^2}{V^2} \delta. \quad (13)$$

The first order AF-F phase transition as shown in Fig. 9 indeed shows the above behavior $(t/\epsilon_f) \sim (t/V)^{1/2} \delta^{1/4}$.

The ferromagnetic local moment likewise can be estimated from the above argument. At density δ of electrons in the conduction band, $N\delta$ of the spins in the

localized levels are bound into singlets, and the remaining ferromagnetic moment per lattice site is given by $m = 2 - n < 1$. This behavior is indeed observed in Fig. 8.

V. CONCLUSION

We have studied the magnetic structure of the ground-state of the symmetric Anderson model on a hypercubic lattice within the manifold of spiral magnetic states, using a slave-boson mean-field approximation. At half-filling ($n = 2$), we find two phases: an antiferromagnetically ordered state, favored among the magnetically ordered states, and the paramagnetic state. The line separating their regions of stability is given by the critical value of the exchange constant $J_c = 4V^2/U \cong 0.036W$. Both phases have a gap in the charge excitation spectrum and are therefore insulators.

For densities less than half-filling incommensurate spiral magnetic order appears. The wave vector of the spiral is found to decrease continuously with decreasing density from $q = (\pi, \dots, \pi)$ (AF order) at $n = 2$ (for $J < J_c$) along the space diagonal of the cubic Brillouin zone to $q = 0$, defining a critical density n_1 . For densities lower than n_1 saturated ferromagnetic order appears in that the localized f -electron spins are ferromagnetically ordered, while the electrons in the conduction band are polarized in the opposite direction, screening part of the ferromagnetic moment, which is thus found to grow linearly with decreasing density. At a second critical density, close to quarter filling ($n = 1$), we find a transition into an antiferromagnetically ordered state. This AF phase is shown to be induced by a higher-order superexchange mechanism, governing the spin dynamics in the insulating state at quarter filling. It thus cannot be found in the Kondo lattice model, which follows from the Anderson model via a Schrieffer-Wolff transformation, and is only valid in lowest order in the hybridization.

The good agreement of our results with quantum Monte Carlo studies at half filling suggests that the phase diagram obtained in this work gives a qualitatively correct picture of magnetic ordering in the PAM.

ACKNOWLEDGMENTS

Partial support by Sonderforschungsbereich 195 der Deutschen Forschungsgemeinschaft and by Landesforschungsschwerpunktprogramm "Grundlagenforschung auf dem Gebiet der Hochtemperatur-Supraleitung" is gratefully acknowledged.

¹ For a review, see P. Fulde, J. Keller, and G. Zwicknagl, *Solid State Physics*, edited by H. Ehrenreich and D. Turnbull (Academic, New York, 1990), Vol. 41, p. 1; H.R. Ott, in *Progress in Low Temperature Physics*, edited by D.F.

Brewer (North-Holland, Amsterdam, 1987), Vol. XI, p. 215.

² P.W. Anderson, *Phys. Rev.* **124**, 41 (1961).

³ S. Doniach, *Physica* **B 91**, 231 (1977).

⁴ A.M. Tselick and P.B. Wiegmann, *Adv. Phys.* **32**, 453

- (1983).
- ⁵ N. Andrei, K. Furuya, and J.H. Lowenstein, *Rev. Mod. Phys.* **55**, 331 (1983).
- ⁶ K.G. Wilson, *Rev. Mod. Phys.* **47**, 773 (1974).
- ⁷ M. Sigrist, H. Tsunetsugu, and K. Ueda, *Phys. Rev. Lett.* **67**, 2211 (1991); M. Sigrist, H. Tsunetsugu, K. Ueda, and T.M. Rice, *Phys. Rev. B* **46**, 13 838 (1992).
- ⁸ M. Troyer and D. Würtz, *Phys. Rev. B* **47**, 2886 (1993).
- ⁹ S.E. Barnes, *J. Phys. F* **6**, 1375 (1976); **7**, 2637 (1977).
- ¹⁰ P. Coleman, *Phys. Rev. B* **29**, 3035 (1984); **35**, 5072 (1987).
- ¹¹ N. Read and D. Newns, *J. Phys. C* **16**, L1055 (1983); **16**, 3273 (1983); D.M. Newns and N. Read, *Adv. Phys.* **36**, 799 (1987).
- ¹² G. Kotliar and A.E. Ruckenstein, *Phys. Rev. Lett.* **57**, 1362 (1986).
- ¹³ T.C. Li, P. Wölfle, and P.J. Hirschfeld, *Phys. Rev. B* **40**, 6817 (1989); R. Frésard and P. Wölfle, *J. Mod. Phys. B* **6**, 685 (1992); **6**, 3087(E) (1992).
- ¹⁴ T.M. Rice and K. Ueda, *Phys. Rev. Lett.* **55**, 995 (1985); *Phys. Rev. B* **34**, 6420 (1986).
- ¹⁵ C.M. Varma, W. Weber, and L.J. Randall, *Phys. Rev. B* **33**, 1015 (1986).
- ¹⁶ B.H. Brandow, *Phys. Rev. B* **33**, 215 (1986).
- ¹⁷ P. Fazekas, *J. Magn. Magn. Mater.* **63&64**, 545 (1987).
- ¹⁸ R.M. Fye and D.J. Scalapino, *Phys. Rev. Lett.* **65**, 3177 (1990).
- ¹⁹ A.M. Reynolds, D.M. Edwards, and A.C. Hewson, *J. Phys. Cond. Matter* **41**, 7589 (1992).
- ²⁰ R. Strack and D. Vollhardt, *Mod. Phys. Lett. B* **2**, 1377 (1991).
- ²¹ W. Brenig and E. Müller-Hartmann, *Ann. Phys.* **1**, 39 (1992).
- ²² Z. Gulasci, R. Strack, and D. Vollhardt, *Phys. Rev. B* **47**, 8594 (1993).
- ²³ R. Blankenbecler, J.R. Fulco, W. Gill, and D.J. Scalapino, *Phys. Rev. Lett.* **58**, 411 (1987).
- ²⁴ P. Fazekas and E. Müller-Hartmann, *Z. Phys. B* **85**, 285 (1991).
- ²⁵ C. Bastide and C. Lacroix, *J. Phys. C* **21**, 3557 (1988).